KSCE Journal of Civil Engineering (2024) 28(6):2304-2314
DOI 10.1007/s12205-024-1183-4

pISSN 1226-7988, eISSN 1976-3808
www.springer.com/12205

Structural Engineering

Axial Compression Tests for Circular Concrete-Filled Steel Tube (CFST) Columns with Notch Imperfection

Mustafa Mohammed[a], **Mustafa Fahmi Hasan**[b,c], **Hasan Fahmi Hasan**[c,d], **Alyaa Assad Mahdi**[c,d], **Sarwar Hasan Mohmmad**[e], **and Mukhtar Hamid Abed**[f,g]

[a]*CLV Group, Ottawa, K1L6V6, Canada*
[b]*Dept. of Construction and Materials Technology Engineering, Erbil Technology College, Erbil Polytechnic University, Erbil 44001, Iraq*
[c]*Dept. of Civil Engineering, Cihan University-Erbil, Kurdistan Region 44001, Iraq*
[d]*Dept. of Computer Science, Cihan University-Erbil, Kurdistan Region 44001, Iraq*
[e]*Technical College of Engineering, Sulaimani Polytechnic University, Sulaymaniyah 46001, Iraq*
[f]*Dept. of Civil Engineering, University of Anbar, Anbar 55431, Iraq*
[g]*Projects Department, Al Ramadi Municipality, Anbar Province, Iraq*

ARTICLE HISTORY

Received 17 June 2023
Revised 4 October 2023
Accepted 13 December 2023
Published Online 20 March 2024

KEYWORDS

Concrete-filled steel tube (CFST)
Stub columns
Column buckling
Notch
Material imperfections
Normal-strength concrete (NSC)
High strength concrete (HSC)

ABSTRACT

The study investigated how simulated notches within concrete-filled steel tube (CFST) columns affect their mechanical performance. It aimed to understand the impact of notch length, orientation, and location within the steel tubes on the behavior of these circular columns. Study conducted compressive tests on a total of 32 CFST specimens, varying in thickness (3 mm and 6 mm) and filled with High-Strength Concrete (HSC) or Normal-Strength Concrete (NSC). Four control specimens without notches served as reference points. Results indicated that CFST columns with notches exhibited reduced mechanical performance compared to those without notches. Notch parameters played a crucial role in this reduced performance. Notch length and orientation had a more significant influence than notch location. It also highlighted that the thickness of the steel tube was a paramount factor, surpassing the importance of concrete type. In summary, the study emphasized that presence of notches in CFST columns significantly impacted their load-bearing capacity, buckling behavior, and failure modes. Length and orientation of notches were identified as critical factors, with steel tube thickness being a dominant factor in determining overall mechanical performance of these columns. These findings provide valuable insights for structural engineers and designers working with CFST columns in various construction applications.

1. Introduction

The justification for using two or more materials together is to get the benefits of the combined material properties and increase their capabilities. Hence, the steel molds were filled with concrete to create a CFST, where CFST merges the concrete properties with the steel properties. Also, the composite of steel and concrete in CFST structures members provides characteristics unavailable in steel or concrete structures separately. Filling the tubes with concrete postpones the steel tubes' buckling, whereas the steel tubes provide limitations for concrete filling (Alfawakhiri, 1997; Tao et al., 2011; Lai et al., 2014). When combined with axial, flexure, and flexural loads, the CFST member's behavior may be more capable than that of reinforced concrete or structural steel members. Additionally, to speed up construction and save costs, steel tubes are used as formwork when pouring concrete (Lai et al., 2014). The CFST is ideal for constructing towers in areas prone to earthquakes. Due to the lack of knowledge on inelastic behaviors and the genuine CFST members' strength, their usage is limited. Also, the performance as a permanent and indispensable framework is one of the advantages of CFST besides providing an external reinforcement system for the concrete supporting ports at several planes of the structure before pumping concrete (Han et al., 2014; Ghannam, 2016). For years, extensive research

CORRESPONDENCE Mustafa Fahmi Hasan mustafa.fahmi@epu.edu.iq Dept. of Construction and Materials Technology Engineering, University of Erbil Polytechnic, Erbil 44001, Iraq

has been undertaken to study the CFST columns' performance. The benefits of concrete and steel appear to have given the CFST columns load capability and good behavior (Han et al., 2014). Works of literature discuss usual columns' mechanical properties and the strength of steel and concrete; moreover, 15 circular CFFST columns were tested to see how they behaved. The criteria investigated were concrete confinement and the connection between the steel tube and concrete with the steel tube wall thickness. Each column's length was 300 mm, and its diameter was 114 mm. Furthermore, concrete had diameter-to-thickness ratios (D/t) ranging from 22.9 to 30.5 with compressive strengths of 30, 60, and 100 N/mm^2. The findings show that the link between concrete and steel tubes increases the CFST columns' strength. Additionally, under peak loads, a tiny shortening, resembling a fracture, emerges at both ends of the notch, which causes substantial displacements for the ultimate load for typical concrete (Giakoumelis and Lam, 2004). The effectiveness of CFST columns was established by (Zeghiche and Chaoui, 2005). 20 CFST columns with a 5 mm wall thickness and a circular CFS with an outer diameter of 160 mm were used. The column ranged in length from 2.0 m to 4.0 m, and each moment measured 500 mm. Concrete infill had strengths of 40, 70, and 100 N/mm^2. The Columns were subjected to various loading patterns (axial-eccentric-bending). The two primary variables examined were the CFST length and concrete strength. The findings demonstrate that the columns' length has an important bearing on their ability to handle more weight by shortening them. Additionally, the concrete's strength was reduced due to the CFST's load-bearing ability increase.

The occurrence of notches in CFT columns can be attributed to erosion and regional cuts that have transpired as a result of environmental and human activities during the design or construction phases. These factors have contributed to localized damage or deformation in the columns (Li et al., 2022). Therefore, the primary emphasis of previous research has been on investigating the impact of notches on the structural integrity and load-bearing capacities of columns. The impact of various notches on the compositional behavior of rectangular CFST columns has frequently been disregarded. Moreover, the existing methods utilized for the determination of the strength of notched columns were sometimes too intricate and demonstrated effectiveness just for columns with certain notch configurations (Ding et al., 2017). Guo et al., (2020) employed an artificial notch to investigate the axial behavior of square concrete-filled steel tubes (CFST) experiencing localized corrosion. Following the suggestions put out by previous researchers, the localized instances of corrosion observed in the pertinent samples were simulated using fake notches. These notches were deliberately created in the steel tubes of the specimens, with variations in their lengths, depths, widths, and orientation angles. Furthermore, a comprehensive investigation was carried out, encompassing several parameters such as the length of the notch, the orientation of the notch, the strength of the concrete, and the ratio of steel. The study's findings revealed that the notched CFT specimens exhibited distinct failure mechanisms compared to the intact CFT specimens. The findings also indicated that the mechanical performance of the notched CFT specimens was inferior to that of the intact CFT specimens. This disparity can be attributed to the inadequate confining effect provided by the notch in the steel tube, which fails to reinforce the concrete core contained therein sufficiently.

The present study aims to discern the impact of material notches on the characteristics of concrete-filled steel tube (CFST) columns. The steel tube specimens underwent precise incisions at varying lengths (50 and 100 mm), orientations (0, 45, and 90 degrees), and positions to emulate artificial notches. Subsequently, the load-bearing capacity of these notched columns was evaluated through compressive testing of CFST columns. Furthermore, an exploration into the flexural performance of steel tube columns filled with both Normal-Strength Concrete (NSC) and High-Strength Concrete (HSC) unveiled that the mechanical behavior of CFST columns with notches exhibited significant deterioration compared to their un-notched counterparts. Each notched column exhibited distinct load-end shortening responses directly correlated with their buckling capacities and failure modes. These outcomes, along with the valuable insights gleaned from this study, hold considerable relevance for future experimental endeavors.

2. Material Properties

2.1 Concrete Properties

In this study, Normal-Strength Concrete (NSC) and High-Strength Concrete (HSC) were the two primary types of concrete employed. Cement (C), Fly Ash (FA), Water (W), Super Plasticizer (SP), Natural Course Aggregate (NCA) with a maximum particle size of 10 mm, Crushed Sand (CS) with a range of particle sizes of 2-0.3 mm and 0.3 mm as finer, and Natural Fine Aggregate (NFA) with a maximum particle size of 4 mm were the components of the NSC mix ratio. The mix design has been conducted for the M30 grade, with a water-to-cement (w/c) ratio of 0.33. The HSC had the same previous components used for the NSC, except this

Table 1. Mix ratio of NSC and HSC

Concert Type	Mix Ratio	C	FA	W	SP	CA	NS	CS 2 – 0.3 mm	CS <0.3 mm	Concrete strength (MPa)
NSC1	Kg/m^3	12.100	12.540	8.276	0.122	31.233	28.63	6.362	3.181	41.63
NSC2	Kg/m^3	12.100	12.540	8.276	0.122	31.233	28.63	6.362	3.181	42.90
HSC1	Kg/m^3	25.960	----	8.276	0.295	36.762	29.410	4.902	2.451	75.60
HSC2	Kg/m^3	25.960	----	8.276	0.295	36.762	29.410	4.902	2.451	74.13

Fig. 1. Concrete Specimens before Crushing under Compression Machine

time, Fly Ash (FA) was added, which was previously abandoned to obtain the required properties for the HSC. The mix proportion of strength concrete and normal strength concrete is given in Table 1. The concrete classification was divided into four days; one mix was cast each day to fill 8 columns and four-cylinder molds to check the concrete strength. On the testing day, the mean compressive strength of the mix percentage is measured in the laboratory for the four cylinders 100 mm by 200 mm, illustrated in Fig. 1 and Table 1.

The crushing test for concrete specimens was carried out using universal testing equipment with a 3,000 kN capacity and load-controlled loading at a rate of 1.5 kN/sec. Sulfur was applied to both ends of each concrete specimen after curing and before testing to guarantee level surfaces. It was necessary to provide correct findings from crushing tests (ASTMC617/C617M-15, 2015).

2.2 Steel Tube Properties

In our study, two different circular steel tube sections were utilized, with 32 columns in total. The first section has a 114.3 mm outer diameter with a steel tube thickness of 3 mm, while the second has a 114.3 mm outer diameter with a 6 mm steel tube thickness. These geometrical properties correspond to two different D/t ratios of 19.05 and 38.1. Considering the practical applications of CFST columns, the studied range of the D/t ratio is highly representative. The yield strengths and stresses for each steel tube were determined by a tensile test to study the mechanical performance of the steel tubes. The tens for each coupon specimen were sectioned for each steel tube with specific dimensions and prepared according to (ASTME8/E8M-16, 2016) requirements, as shown in Fig. 2. The yield strengths and ultimate stresses were measured and given in Table 2, and the elastic modulus is equal to 200 GPa.

2.3 Preparation of CFST Columns

The preparation of columns started with cutting the steel tube purchased to get the local market with a fixed length of 6 m for the required length for specimens (343 mm). To evenly distribute the applied load along the cross-section where the concrete and steel are loaded simultaneously, both ends of the specimens were

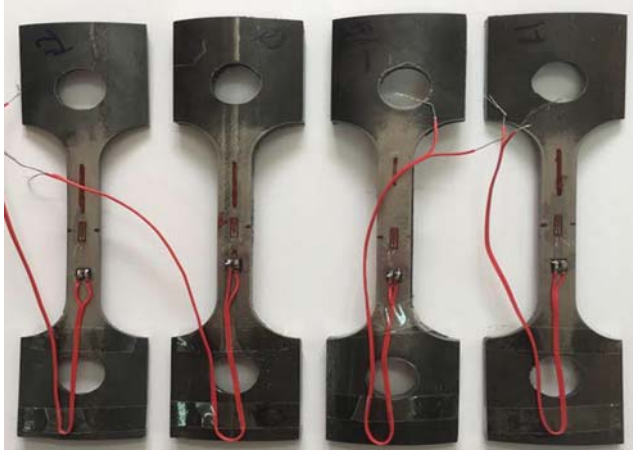

Fig. 2. Tensile Coupon Specimens

Table 2. The Mechanical Properties of the Steel Tubes

Tube cross section (mm)	Yield strength (Fy) (MPa)	Ultimate strength (Fu) (MPa)
3	435	649
6	348	576

machined to achieve the same level for the ends surfaces. The hollow steel tube specimen underwent machining treatment to create notch patterns before the concrete was poured. The specimen has undergone this machining process, a crucial step in obtaining accurate test findings. The ones that were produced were regarded as CFST material flaws. As seen in Fig. 3, a Descartes coordinate system was employed. The x-axis and the y-axis were oriented towards the steel tube's generator, and their respective axes' centers were situated at the steel tube's midway height. They both pointed at the tangent of the outside.

The notches were described precisely depending on many main terms like the notch size (length of the arc between the two points of the end, which is between 50 mm and 100 mm (l) and width (b)), orientation (θ), and the location of the notch. The depth of the notch was fixed because it was connected directly to

the thickness of the steel tube itself (3 mm, 6 mm). Also, the notch was fixed in the center of the origin coordinates of the steel tube to decrease the numerous amounts of variables. The length of the notch was known as the length of the arc between the two points of the end of the incision, and it was 50 mm and 100 mm. The definition of the orientation of a notch was the angle enclosed between the y-axis along the tube and the x-axis in the center of the tube. In our case study, there were three orientations for the notch: 90º right angles on the x-axis, 45º and 0º.

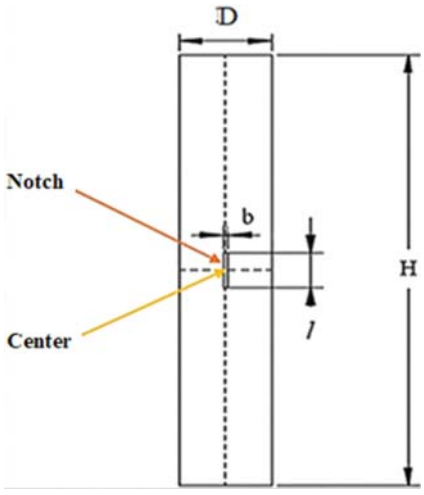

Fig. 3. Sketch for the Notch Location

In contrast, there were two main locations of the notch, the first at the center of the weld line of the tube and the second on the opposite side of the weld line. The performance of the steel tube is affected by the rectangular notch due to the high-stress concentration that could presumably exist near the corners of the notch, which may lead to sharp discontinuities in the steel tube body of the CFST columns. Thirty-two specimens were built and examined, including four control specimens with no notches and 28 specimens with artificial notches with varying notch characteristics, including orientation position and size. Tables 3 and 4 include a complete set of sample-related information. After being dust-free, the steel tube is oiled with a dry cloth. Steel and

Table 3. Properties of Column Specimens with 3 mm Thickness

Group	Specimen	Orient (θ)	Location	$l \times b$ (mm)	Next	D/t	L/D	Fc (MPa)	Fy (MPa)	N_{exp} (kN)
One	NC-3-C	-	-	-	114.3 × 3 × 343	38.1	3	41.63	435	1005
	NC-3-H-50	0º	Opposite	50 × 5	114.3 × 3 × 343	38.1	3	41.63	435	982
	NC-3-H-100	0º	Opposite	100 × 5	114.3 × 3 × 343	38.1	3	41.63	435	971
	NC-3-D-100	45º	Opposite	100 × 5	114.3 × 3 × 343	38.1	3	41.63	435	872
	NC-3-V-100	90º	Opposite	100 × 5	114.3 × 3 × 343	38.1	3	41.63	435	860
	NC-3-V-50	90º	Opposite	50 × 5	114.3 × 3 × 343	38.1	3	41.63	435	904
	NC-3-V-W-50	90º	Weld line	50 × 5	114.3 × 3 × 343	38.1	3	41.63	435	891
	NC-3-V-W-100	90º	Weld line	100 × 5	114.3 × 3 × 343	38.1	3	41.63	435	830
Two	HC-3-C	-	-	-	114.3 × 3 × 343	38.1	3	75.60	435	1366
	HC-3-H-50	0º	Opposite	50 × 5	114.3 × 3 × 343	38.1	3	75.60	435	1358
	HC-3-H-100	0º	Opposite	100 × 5	114.3 × 3 × 343	38.1	3	75.60	435	1394
	HC-3-D-100	45º	Opposite	100 × 5	114.3 × 3 × 343	38.1	3	75.60	435	1263
	HC-3-V-100	90º	Opposite	100 × 5	114.3 × 3 × 343	38.1	3	75.60	435	1193
	HC-3-V-50	90º	Opposite	50 × 5	114.3 × 3 × 343	38.1	3	75.60	435	1295
	HC-3-V-W-50	90º	Weld line	50 × 5	114.3 × 3 × 343	38.1	3	75.60	435	1293
	HC-3-V-W-100	90º	Weld line	100 × 5	114.3 × 3 × 343	38.1	3	75.60	435	1180

Table 4. Properties of Column Specimens

Group	Specimen	Orient (θ)	Location	$l \times b$ (mm)	$D \times t \times H$ (mm)	D/t	N_{ext}	Fc (MPa)	Fy (MPa)	N_{exp} (kN)
Three	NC-6-C	-	-	-	114.3 × 6 × 343	19.05	3	42.90	348	2254
	NC-6-H-50	0º	Opposite	50 × 5	114.3 × 6 × 343	19.05	3	42.90	348	2256
	NC-6-H-100	0º	Opposite	100 × 5	114.3 × 6 × 343	19.05	3	42.90	348	2273
	NC-6-D-100	45º	Opposite	100 × 5	114.3 × 6 × 343	19.05	3	42.90	348	2056
	NC-6-V-100	90º	Opposite	100 × 5	114.3 × 6 × 343	19.05	3	42.90	348	2080
	NC-6-V-50	90º	Opposite	50 × 5	114.3 × 6 × 343	19.05	3	42.90	348	2205
	NC-6-V-W-50	90º	Weld line	50 × 5	114.3 × 6 × 343	19.05	3	42.90	348	2223
	NC-6-V-W-100	90º	Weld line	100 × 5	114.3 × 6 × 343	19.05	3	42.90	348	2098

Fig. 4. Column Specimens

concrete can interact successfully thanks to the cleaning within the steel tube. To reduce the adhesion between the concrete surface and base plate, silicon was applied to attach the mica plates to the bottom of the steel tubes while pouring the concrete concrete. This process ensured that a flat concrete surface could be easily created at the bottom end when the mica plates were removed. Silicon was used within the notch to prevent the leakage of concrete from the tubes into the notch during the casting process, followed by the application of adhesive tape. The silicon was removed from the notch, and the mica plate was removed from the tube end after the concrete had dried. The final 5 mm section was left unfilled and levelled using high-strength levelling epoxy during the concrete pour. This two-component epoxy-based repair, anchoring, and adhesive mortar ensures that the load will be distributed evenly across the whole section. When the samples are prepared for testing, one end is capped with epoxy to prevent moisture loss during curing. The thirty-two CFST columns are ready for testing after being cleaned on their outside surfaces, as illustrated in Fig. 4.

The following system of remarking each tube in Tables 3 and 4 was designated with a specific meaning for each name, and it includes concrete type, steel tube thickness t, notch orientation (θ), the notch location, and notch length (l), respectively. For example, the specimen (HC-6-V-W-50) refers to a normal strength concrete core (NC) with a 6 mm thickness of steel tube, a vertical notch with 90º, (W) refers to the location of the notch in the weld line, and the notch length is 50 mm The specimen designation (NC-6-C) stands for control without notch. In comparison, NC refers to standard strength concrete for the core and 3 mm steel tube thickness.

The mica plates were dismounted from the lower base of the column before the laboratory test; also, the lower base was cleaned from silicon residues. When the models were placed in the testing machine, they were carefully placed to avoid the tolerance of eccentric loading and associated bending effect. As shown in Fig. 5, the technique was followed with all specimens

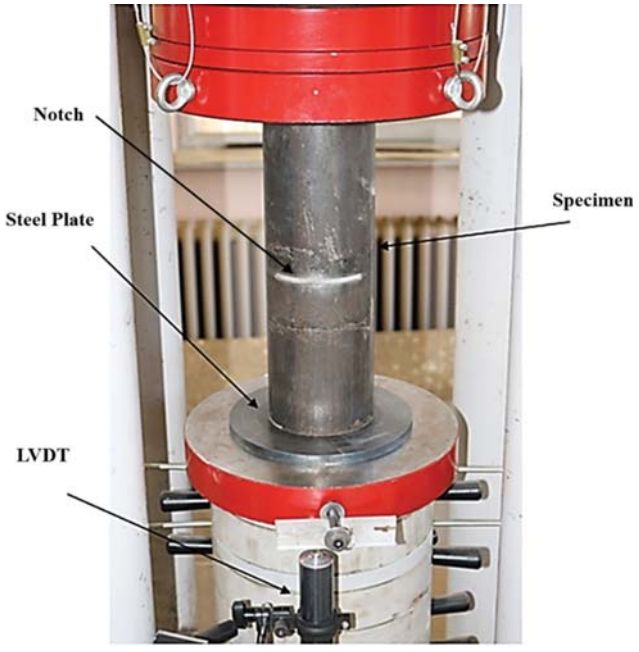

Fig. 5. Column's Specimen under Compression Machine Test

after inserting them into the testing apparatus and gradually increasing the displacement at a set rate of 0.5 mm/min until the test was complete. By comparing compression loading (KN) versus displacement (mm) data, the pre- and post-collapse points of the CFST column have been found and documented for the column's behavior at those moments to examine its performance.

3. Results and Discussion

All test findings were documented throughout the duration of the test, up until its completion, with the exception of the specimens containing high-strength concrete with a steel tube thickness of 6 mm. The specimens were excluded from the analysis due to their excessive strength, which exceeded the capacity of the testing equipment to crush them. This was attributed to the high characteristics of the concrete and steel tube used in their construction.

3.1 Failure Modes

After the test, the failure modes will be explored while considering the columns' behavior because all columns have a significant stiffness capacity. After the test, CFST columns with the notch collapsed due to the local failure of the steel tube (external buckling) and notch failure (steel defects). Local concrete crushing and accompanying failure modes follow outward local buckling of the steel tubes (Zhu et al., 2021). The test results indicated that narrow columns commonly exhibited a mode of failure that significantly impairs their structural integrity (Ding et al., 2017). The samples may be broken down into a variety of common failure scenarios. As shown in Fig. 6, the first group was constructed using standard-strength concrete and a 3 mm thick steel tube segment. Under an axial compression force, the

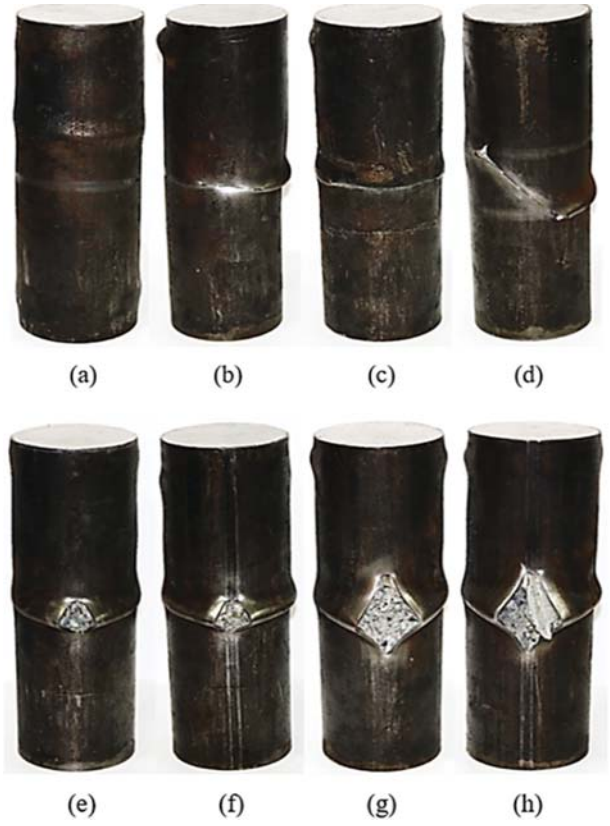

Fig. 6. Typical Failure Modes for Test Specimens: (a) NC-3-C, (b) NC-3-H-50, (c) NC-3-H-100, (d) NC-3-D-100, (e) NC-3-V-50, (f) NC-3-V-W-50, (g) NC-3-V-100, (h) NC-3-V-W-100

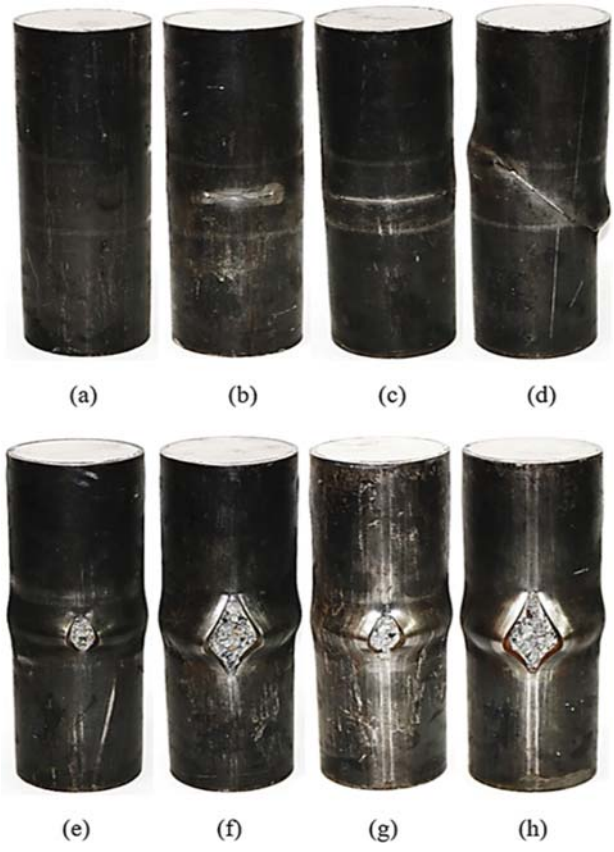

Fig. 7. Typical Failure Modes for Test Specimens: (a) NC-6-C, (b) NC-6-H-50, (c) NC-6-H-100, (d) NC-6-D-100, (e) NC-6-V-50, (f) NC-6-V-W-50, (g) NC-6-V-100, (h) NC-6-V-W-100

sample with a 50 mm notch in the middle of the horizontally oriented tube invariably closes. The specimen NC-3-H-50 had outward local buckling near a distance from the top of the column and at the center beside the notch and noticeable compression failure for the concrete at the center. The specimen NC-3-H-100 shows less effect of the outward local buckling at both locations due to the equal compression failure of the concrete. In addition, all the samples with vertical notches NC-3-V-50, NC-3-V-100, NC-3-V-W-50, and NC-3-V-W-100 show a noticeable outward local buckling at the center of the columns beside the end of the notch and minor outward local buckling at a distance from the top end of the columns at the end of the test. The present investigation yielded a notable distinction in the failure modes between notched CFST columns and intact CFST columns when subjected to compressive forces. The prevalent failure modes observed were characterized by bulging and the subsequent closure of the notch. The failure modes observed in this study were closely associated with the orientation of the notches. Specifically, specimens with a horizontal notch exhibited failure through the closure of the notch, while specimens with a vertical notch experienced failure through bulging the notch (Ding et al., 2017).

For the third columns group, normal strength concrete was used, and a thick steel tube section of 6 mm thickness, as indicated in Fig. 7. The samples with 50 mm and 100 mm notch lengths at the center of the tube with horizontal orientation are always closed under axial compression load and specimens show a minor outward local buckling at the center beside the notch because of the thicker section of the steel that prevents concrete spalling and provides concrete confinement. In addition, all the samples with vertical notch NC-6-V-50, NC-6-V-100, NC-6-V-W-50, and NC-6-V-W-100 show only a noticeable outward local buckling at the center of the columns beside the notch at the end of the test. The specimen NC-6-D-100 with a diagonal notch orientation of 45º shows similar behavior to specimen NC-3-D-100 for the failure mode, except the outward local buckling only exists at both ends of the notch. In one particular specimen, NC-6-V-W-50, cracks were observed exclusively at both ends of a 50 mm vertical notch at the weld line. This phenomenon was not observed in the other specimens with vertical notches. It is plausible to attribute this occurrence to the elevated ductility of the steel tube (Ding et al., 2017). According to experimental findings, local outward buckling is the common failure mode for steel tubes. Concrete in-filled shear failure is related to local buckling of the round-ended steel tube. The ductility of the specimen reduces for CFRT stub columns as the D/t ratio increases. The larger D/t ratio of the CFRT stub columns appears to have an inadequate constraining impact on the concrete core inside (Faxing et al., 2015).

The construction of the third group involved the utilisation of high-strength concrete in conjunction with a steel pipe segment

Fig. 8. Typical Failure Modes for Test Specimens: (a) HC-3-C, (b) HC-3-H-50, (c) HC-3-H-100, (d) HC-3-D-100, (e) HC-3-V-50, (f) HC-3-V-W-50, (g) HC-3-V-100, (h) HC-3-V-W-100

possessing a thickness of 3 mm. Upon the application of an axial compressive force, the specimen, which consists of a horizontally oriented tube with a centrally located notch measuring 50 mm, undergoes permanent closure. The observed behaviour of specimen HC-3-H-50 is characterised by the occurrence of localised outward buckling, which is observed at a certain distance from the top of the column and in the central region adjacent to the notch. The concrete located at the centre exhibits notable compression failure. The HC-3-H-100 specimen exhibits a reduced occurrence of outward local buckling at both places. The aforementioned phenomenon can be attributed to the identical compressive failure of the concrete material. Furthermore, it is seen that all HC-3-V-50, HC-3-V-100, HC-3-V-W-50, and HC-3-V-W-100 vertical notch specimens exhibit pronounced outward local buckling in the central region of the columns adjacent to the notch termination. Additionally, these specimens display modest instances of external local buckling at a certain distance from the top of the columns towards the end of the testing process. As seen in Fig. 8.

3.2 Effect of the Test Parameters

3.2.1 Length of Notch

It is convenient to classify the column specimens considering the length of the notch. Fig. 9(a) clearly demonstrates the influence of notch length on the samples, specifically the NC-3-H-50 and NC-3-H-100, which exhibited peak loads of 979 and 970 kN, respectively. During the elastic phase, a noticeable distinction was observed in the behaviour of the columns with a notch length of 100 mm, as they exhibited an early yield peak compared to the columns with a 50 mm notch length, with yield points recorded at 815 and 664, respectively. Fig. 9(b) indicates the relation of

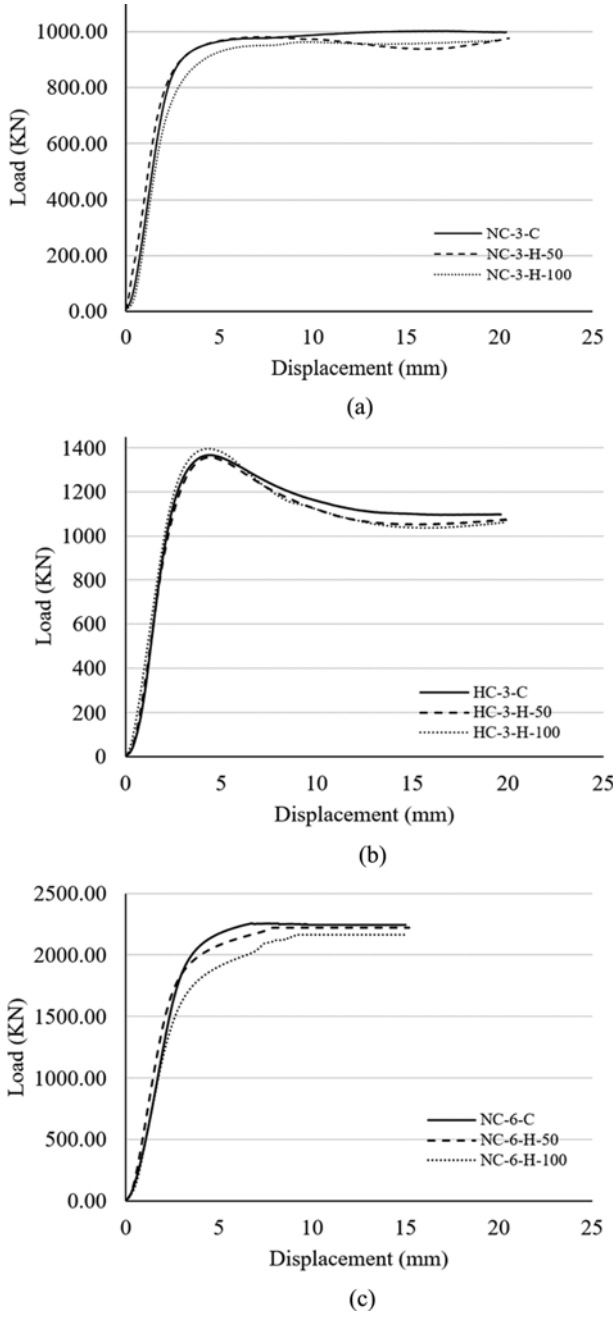

Fig. 9. Variation of Load-Displacement Response Curve according to Notch Length: (a) and (b) Normal and Strength Concrete with the Horizontal Notch of 3 mm Steel Thickness, (c) Normal Strength Concrete with the Horizontal Notch of 6 mm Steel Thickness

compression loading versus displacement curves for the specimens HC-3-V-50 and HC-3-V-100, which were similar to the concrete type, the thickness of the steel tube, and the orientation of the notch, except in the length of the notch which was 50 mm and 100 mm respectively. In the elastic stage of the failure load, the curve is not affected by the notch length for each specimen until it reaches its yield point. The elastic stage was longer for the control specimen compared to the specimen with a notch, and even depending on the length of the notch, the short notch shows a longer elastic stage than the long one. The peak loads were 1295.39 and 1193.01 kN, respectively. The corresponding displacements increased from 2.99 to 3.48 mm, and the impact of the length appears there. Therefore, with the increase of the notch length, the columns' mechanical performance will decrease in any case. The research revealed that specimens with longer slanted notches exhibited a decrease in peak resistance. In contrast to the specimens including slanted notches, the variable's impact on the peak specimen resistance is comparatively less pronounced in the specimens incorporating horizontal notches. This phenomenon is because a specimen with a longer slanted notch results in a longer tube segment, which in turn provides inadequate confinement for the concrete fill. Therefore, this leads to a decrease in the peak resistance exhibited by the specimen (Huang et al., 2021), which occurred with all similar cases in this study. Regardless of the type of concrete, the thickness of the steel tube or even the orientation of the notch appears distinctly in Fig. 9(c). The specimens affected by the notch length were NC-6-H-50 and NC-6-H-100 with peak loads 2,225 and 2,165 kN, respectively. In the elastic stage, there was a clear difference in the behavior of columns with 100 mm notch length, which had early yield pick compared to the 50 mm notch pick load at yield points 1239 and1770. The behavior of the columns in the plastic stage has been different for these columns. The proximity in curves at the end of the plastic stage was because of the effect of steel tube thickness and sealing of the horizontal notch because of the axial load. The influence of the expansion notch length can lead to lower peak load and corresponding displacement. Therefore, it should be noted that in the samples including horizontal notches in the steel tubes, the size of the horizontal notch does not impact the length of the tube segment, which ultimately results in inadequate confinement for the concrete fill. Therefore, the peak resistance of the specimen with the horizontal notch exhibits reduced sensitivity to variations in the length of the notch (Huang et al., 2021). Compared with the literature studies, the final axial-strength calculation method for the notched rectangular CFST columns was suggested based on the parametric research and regression analysis. A coefficient of (1.2 -0.2 sinØ) that could account for the impact of notch inclination angles and lengths was used to characterize the confinement effect of square steel tubes with notches. The simple formula had shown high agreement with test findings and numerical outcomes (Li et al., 2022).

3.2 Location of Notch

Regarding the location of the notch, the result of the load-displacement curve demonstrates the effect of the location and the effect of the notch length, as indicated in Fig. 10. The vertical 90º notch had similar concrete-steel properties. The length of the notch was different in terms of notch location, which was in the center of the weld line for specimen NC-3-V-W-100 and on the opposite side for NC-3-V-100. In the elastic stage of the curve, the columns behave similarly until they reach the yield point and their peak load point, which record 830 and 860 kN, respectively. The corresponding displacements increased from 2.38 mm to 3 mm and approved the effect of the notch's location on the columns' mechanical properties. Also, Fig. 10 indicated similar behavior for the specimens NC-3-V-W-50 and NC-3-V-50. Compared to the study conducted by Ding et al. (2017), it was determined that no significant disparities were identified in the peak loads. However, the reason for this was that the corner confining effect was superior to that of the sidewall in the case of the CFST stub column. Moreover, the presence of a notch in the corner would considerably diminish the confining effect of the steel tube on the core concrete for specimens exhibiting a vertical notch situated within the sidewall and corner. According to the (Li et al., 2022) study, The effects of the diagonal vertical and horizontal notches on the development of axial-column-strength, the composite effect, and the bearing modes in the concrete core were all distinct. The horizontal notch could decrease the steel tube's load participation ratio. Axial column strengths also reduced as the length of the notches increased because the core concrete's stress states changed from the axially loaded mode to the eccentric compression mode. The vertical notch had no discernible impact on the axial column strength. The tube plates around the notch bent in the last stages of strength loss due to considerable axial compressive distortion. Because their influence was intermediate between that of the vertical and horizontal notches, the influence of diagonal notches has been comparable to that of horizontally notched columns with the notch length equal to the horizontal projection length of the diagonal notch (Li et al., 2022).

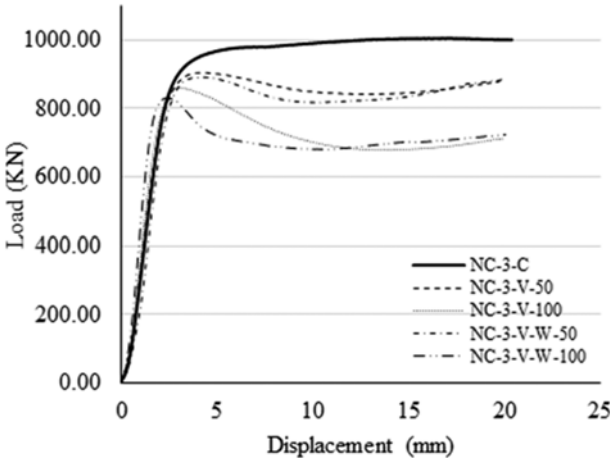

Fig. 10. Notch Location's Effects on the Load-Displacement Response Curve

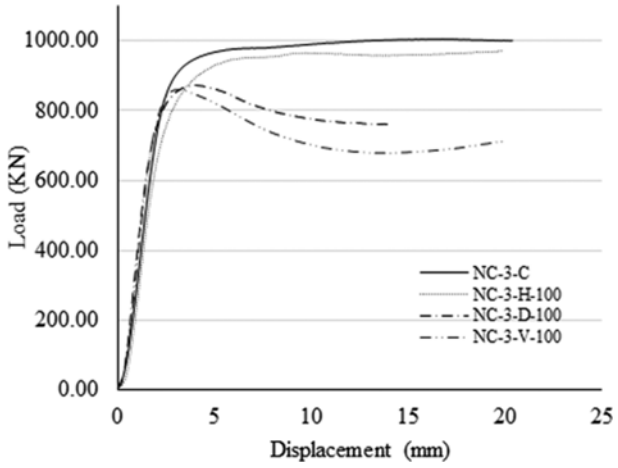

Fig. 11. Variation of Load versus Displacement Curve

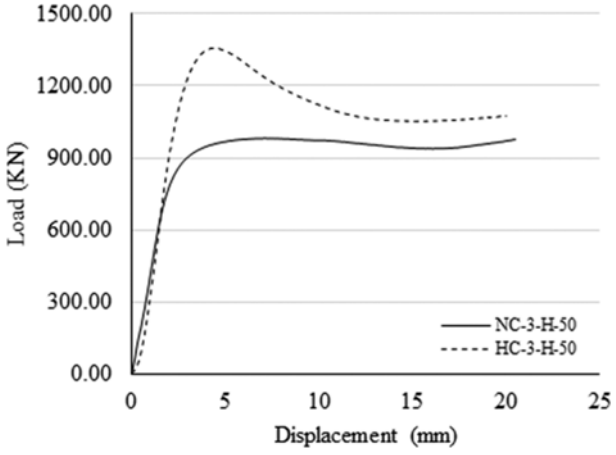

Fig. 12. Effect of the Concrete Strength on the Load-Displacement Response Curve

3.2.3 Orientation of Notch

Figure 11 displays the effect of the orientation on the load-displacement response. When all the parameters for the notched steel tube columns were the same, keeping the orientation variable for specimens NC-3-H-100, NC-3-V-100, and specimen NC-3-D-100 0º for the horizontal notch, 90º for the vertical notch, and 45º for the diagonal notch, respectively. The horizontal 0º notch showed preferable behavior with a higher peak load at the yield point than the vertical 90º, which showed minimal peak load at the yield point. The diagonal notch with 45º was lower than the horizontal and upper than the vertical notch at the yield point of the load-displacement curve with peak loads of 971, 860, and 872 kN, respectively. The impact on the corresponding displacements decreased from 5.25 to 3.00 mm for the horizontal to the vertical and 3.95 mm for the diagonal. The previous results elucidate an effective role for the orientation, especially when the angle is between 45º and 90º. It was understood as a significant decrease in the performance of the columns significantly. Whether the notch orientation was horizontal or vertical, specimens exhibiting identical notch area and position achieved equivalent maximum strain values. According to (Zhu et al., 2021), it can be observed that the damage mechanisms exhibited variations among the notched specimens to some degree. In comparison to the study conducted by Ding et al. (2017), the placement and direction of the notch had a role in the concrete core's collapse. Clear concrete damage could be seen only close to the vertical notches on specimens with corners cut out. Other times, seeing any concrete damage close to the notches is impossible.

3.2.4 Concrete Strength

Regarding the concrete strengths' effectiveness on load-displacement response, a fixed notch length specimen, notch orientation, and other parameters were kept the same. The concrete strength was left variable to assess its influence on the properties of CFST columns. Fig. 12 gave the load-displacement responses for notched specimens NC-3-H-50 and HC-3-H-50, and the variable was the concrete strength with 41.63 and 75.60 MPa, respectively. The columns' strength increased from 981.50 kN to 1357.91 kN for NC-3-H-50 and HC-3-H-50 by increasing the concrete strength. This has been referred to in many other CFT columns without notches studies. The main factors influencing the N/Nu-M/Mu relationship curves of concrete with high strength filled square steel tubular columns with inner CFRP circular tube (HCFSTF) members exposed to bi-axial eccentric loading, according to parametric studies conducted by Li et al., in 2013, are the steel yield strength, concrete strength, steel ratio, and slenderness ratio. The HCFSTF members' N-M interaction curves under bi-axial eccentric stress and with various concrete strengths. The parameters for these samples are FY = 291 Mpa, size of section side for square steel tube (B) = 200 mm, and eccentric angle of 45°. With increasing concrete strength, the inflection point's abscissa (M/Mu) values on the N-M interaction curve rise. The interaction curve is little affected by concrete strength (Li et al., 2013).

3.2.5 Steel Yield Strength

Several previous studies have investigated the impact of steel yield strength on CFST members' behavior. The notched CFST column specimens NC-3-V-W-100 and NC-6-V-W-100 had similar parameters for the notch and the material, except the yield strength was 435 and 348 MPa, respectively, which can be understood that it is commonly observed that the ratio of width to thickness in steel plate tends to exhibit an inverse relationship with the square root of its yield strength. These rules may substantially hinder the utilization of high-strength steel in practical structural elements, as the required thickness of the steel plate would need to be designed excessively thick compared to plates made of standard-strength steel (Ratio et al., 2013). The peak loads were 830.21 and 2098.11 kN, respectively. The corresponding displacements increased from 2.40 mm to 5.37 mm, as shown in Fig. 13. It could be seen that higher yield strength led to higher bear capacity for the columns. The parametric analysis's findings indicate that although increasing concrete strength along with CFRP layers can somewhat enhance bearing capacity, increasing

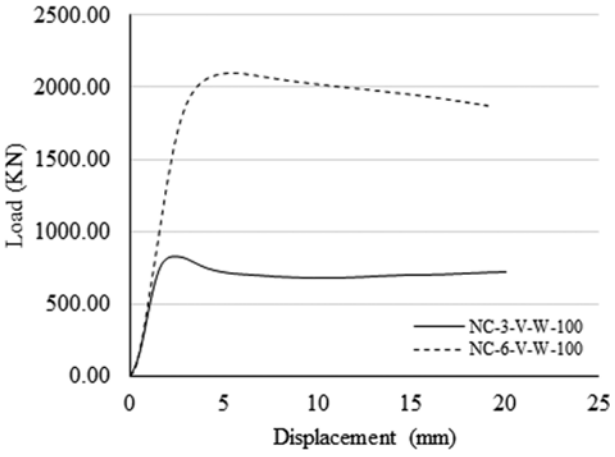

Fig. 13. Effect of the Steel Yield Strength on the Load-Displacement Response Curve

steel yield strength along with steel ratio can greatly raise it. The members' bearing capacity and elastic stiffness dramatically drop with a rise in the slenderness ratio or axial compression ratio, and the load-deformation curve's shape also obviously changes (Wang et al., 2022).

4. Conclusions

This paper presents the results of a study that examined the buckling capabilities of short CFST columns with steel tube notches. This study investigates the conventional strength and flexural behavior of steel tube columns filled with normal and high-strength concrete while maintaining a length-to-diameter ratio (L/D) of 3. The CFST exhibits notches positioned at the midpoint of its height, with three distinct orientations. These notches are available in two different lengths, namely 50 mm and 100 mm, and are designed to accommodate two different thicknesses of steel tubes. The load-end shortening reactions, buckling capacities, and failure processes were enumerated and analyzed. Based on the results obtained from the experiment, it is possible to draw the following conclusions:

1. The collapse of CFST columns can be attributed to two main factors: local failure of the steel tube, specifically external buckling, and notch failure resulting from steel flaws. The primary failure mechanisms seen in notched CFST columns were characterized by outward local buckling near the top of the specimen and at the mid-height positions located at both ends of the notch. The occurrence of local buckling might vary depending on the thickness of the specimen. In the case of a steel tube specimen, a thickness of 6 mm is associated with mild local buckling, while a thickness of 3 mm is associated with severe local buckling.
3. The most effective notches were vertical 100 mm length located at the mid-height of the weld line and the diagonal 45º with 100 mm length. These notches registered the lowest load compression compared with other locations of the notch, lengths, and orientations. Simultaneously, all the columns with vertical notches in the mid-height of the welding line of the tube only and the diagonal notch failed by cracking the end of the notch in the failure mode.
3. The notch location exhibited variation with respect to the length of the notch. Specifically, for specimen NC-3-V-W-100, the notch was positioned at the center of the weld line, but for NC-3-V-100, the notch was situated on the opposite side. During the curve's elastic phase, the columns' behavior is comparable until they reach the yield point and their maximum load point.
4. The notch oriented horizontally at 0º exhibited more desirable characteristics, displaying a higher peak load at the yield point than the vertically oriented notch at 90º, demonstrating minimal peak loads at the yield point. At the yield point of the load-displacement curve with peak loads, the diagonal notch with a 45º angle was observed to be positioned lower than the horizontal notch and higher than the vertical notch.
5. The variability in concrete strength was maintained to evaluate its impact on the characteristics of CFST columns. This study presents the load-displacement responses of notched specimens NC-3-H-50 and HC-3-H-50, with varying concrete strengths of 41.63 and 75.60 MPa, respectively. The columns' strength increased from 981.50 kN to 1357.91 kN for the NC-3-H-50 and HC-3-H-50 specimens, respectively, as a result of augmenting the concrete strength.
6. The thickness of the steel tube and had a distinguished role compared with the concrete type or strength. The thicker steel tube with the same parameters had more than 60% compression load capacity than the thinner steel tube in the weakest case. In comparison, the strength of the concrete increased the compression load capacity for the high-strength concrete specimen by 29% compared to normal-strength concrete in the weakest case. On the other hand, Yield strength was less affected than steel thickness, which varied from 348 to 435 MPa.
7. Future research will provide additional information regarding the findings, which will need to be compared with the results obtained through finite element analysis (FEA). Furthermore, it is advisable to employ a consistent parametric analysis approach in which an artificial notch is introduced at the midpoint of the steel tube, with varying lengths (50 and 100 mm), orientations (0º, 45º, and 90º), and positions, to examine the alterations in mechanical characteristics.

Acknowledgments

Not Applicable

ORCID

Mustafa Mohammed http://orcid.org/0000-0002-4713-3252
Mustafa Fahmi Hasan http://orcid.org/0000-0002-8544-7017
Hasan Fahmi Hasan http://orcid.org/0000-0001-6095-5560
Alyaa Assad Mahdi http://orcid.org/0000-0001-6906-7092

Sarwar Hasan Mohmmad http://orcid.org/0000-0002-7249-7760
Mukhtar Hamid Abed https://orcid.org/0000-0002-8940-8533

References

Alfawakhiri F (1997) Behavior of high strength concrete filled circular steel tube beam-columns. University of Ottawa, Canada

ASTM:C617/C617M-15 (2015) Standard practice for capping cylindrical concrete specimens, ASTM International, West Conshohocken, PA., USA

ASTME8/E8M-16 (2016) Standard test methods for tension testing of metallic material ASTM International. West Conshohocken, PA 19428-2959, USA

Ding F, Wen B, Liu X, Wang H (2017) Composite action of notched circular CFT stub columns under axial compression. *Steel and Composite Structures, An International Journal* 24(3):309-322, DOI: 10.1016/j.tws.2017.02.018

Faxing D, Lei F, Zhiwu Y, Gang L (2015) Mechanical performances of concrete-filled steel tubular stub columns with round ends under axial loading. *Thin-Walled Structures* 97:22-34, DOI: 10.1016/j.tws.2015.07.021

Ghannam S (2016) Flexural strength of concrete-filled Steel tubular beam with partial replacement of coarse aggregate by granite. *International Journal of Civil Engineering and Technology* 7(5)

Giakoumelis G, Lam D (2004) Axial capacity of circular concrete-filled tube columns. *Journal of Constructional Steel Research* 60(7): 1049-1068, DOI: 10.1016/j.jcsr.2003.10.001

Guo L, Huang H, Jia C, Romanov K (2020) Axial behavior of square CFST with local corrosion simulated by artificial notch. *Journal of Constructional Steel Research* 174:106314, DOI: 10.1016/j.jcsr.2003.10.001

Han L-H, Li W, Bjorhovde R (2014) Developments and advanced applications of concrete-filled steel tubular (CFST) structures: Members. *Journal of Constructional Steel Research* 100:211-228, DOI: 10.1016/j.jcsr.2014.04.016

Huang H, Guo L, Qu B, Jia C, Elchalakani M (2021) Tests of circular concrete-filled steel tubular stub columns with artificial notches representing local corrosions. *Engineering Structures* 242(May): 112598, DOI: 10.1016/j.engstruct.2021.112598

Lai Z, Varma AH, Zhang K (2014) Noncompact and slender rectangular CFT members: Experimental database, analysis, and design. *Journal of Constructional Steel Research* 101:455-468, DOI: 10.1016/j.jcsr.2014.06.004

Li B, Ding F, Yu Y, Zhang J, Huang Q, Gong C, Wang H (2022) Research on confinement effect of the outer steel tube in notched square CFST columns. *Materials* 15(15):5161, DOI: 10.3390/ma15155161

Li GC, Yang ZJ, Lang Y, Fang C (2013) Behaviour of high strength concrete filled square steel tubular columns with inner CFRP circular tube under bi-axial eccentric loading. *Advanced Steel Construction* 9:231-246

Ratio W, Hong G, Kim W, Choi I, Chung K (2013) Structural performance of high strength concrete filled steel tube with the structural performance of high strength concrete filled steel tube with the width-to-thicknessratio. September 2014, DOI: 10.4028/www. scientific.net/AMM.284-287.1390

Tao Z, Uy B, Liao F-Y, Han L-H (2011) Nonlinear analysis of concrete-filled square stainless steel stub columns under axial compression. *Journal of Constructional Steel Research* 67(11):1719-1732, DOI: 10.1016/j.jcsr.2011.04.012

Wang Q, Peng K, Guo Y-H, Shao Y (2022) Experimental study on hysteretic behavior of concrete-filled square carbon fiber-reinforced polymer steel tubular beam-column. *ACI Structural Journal* 119(3): 67-80, DOI: 10.14359/51734491

Zeghiche J, Chaoui K (2005) An experimental behaviour of concrete-filled steel tubular columns. *Journal of Constructional Steel Research* 61(1):53-66, DOI: 10.1016/j.jcsr.2004.06.006

Zhu H, Zhang H, Liu L (2021) Experimental study on cyclic lateral loaded circular CFST Members with initial imperfections. *KSCE Journal of Civil Engineering* v25(8)3064-3074, DOI: 10.1007/s12205-021-1931-7